School of Pharmacy[1], Liaoning University, Shenyang; Department of Clinical Laboratory[2], Affiliated Hospital of Guilin Medical University, Guilin; School of Life Sciences[3], Liaoning University; Research Center for Computer Simulating and Information Processing of Bio-Macromolecules of Liaoning Province[4]; Technology Innovation Center for Computer Simulating and Information Processing of Bio-Macromolecules of Shenyang[5], Shenyang, China

Synthesis of sustained release/controlled release nanoparticles carrying nattokinase and their application in thrombolysis

Shuai Liu[1,#], Junfeng Zhu[2,#], Chang Liu[1], Jiazeng Li[3], Li Zhang[3,4], Jian Zhao[3], Hongsheng Liu[1,4,5,*]

Received October 31, 2020, accepted January 16, 2021

**Corresponding author: Hongsheng Liu, School of Pharmacy, Liaoning University, Shenyang 110036, China*
liuhongsheng@lnu.edu.cn
#These authors contributed equally to this work

Pharmazie 76: 145-149 (2021) *doi: 10.1691/ph.2021.0155*

Thrombus-related diseases have a high mortality rate and are seriously threatening human life and health. Nattokinase (NK), which has a strong thrombolytic effect, can treat thrombotic diseases. In this study, NK-conjugated magnetite nanoparticles (NK-MNPs) were prepared to accurately deliver NK to the thrombus site. Fe_3O_4, carboxymethyl chitosan and sodium alginate were combined to form magnetite nanoparticles (MNPs), which were prepared to encapsulate NK. The mean diameter of NK-MNPs was 168.9±4.8 nm, and the zeta potential was -33.8±0.9 mV. The release percentage reached a plateau in approximately 12 h, with 65.24% NK released. Magnetic targeting experiments showed that the light transmittance of the solution reached 90%. The results from the *in vitro* thrombolysis experiments demonstrated the sustained release thrombolysis potential of NK-MNPs. A hemolysis experiment demonstrated that the hemolysis rate of NK-MNPs was less than 5% at an enzymatic activity of 50–150 IU/mL. Moreover NK-MNPs were stored for 90 days at 4 °C and still maintained an enzyme activity above 90%. In conclusion, NK-MNPs hold great promise for improved thrombolytic efficacy, with sustained release and magnetic targeting.

1. Introduction

The incidence of thrombotic diseases is increasing year by year, which seriously threatens people's lives and health (Baaten et al. 2018; Wu et al. 2019). Thrombosis is the accumulation of blood vessel contents such as fibrin, platelets, white blood cells, and red blood cells into a clot, which prevents the normal circulation of blood (Lee et al. 2017a; Bourcier et al. 2017b). Blood is a medium for the body to absorb nutrients and eliminate metabolites. Accordingly, the formation of blood clots can cause poor blood flow and affect the transport of nutrients and metabolic waste. Tissues and organs that cannot be supplied with normal nutrients gradually fail and develop lesions (Govindarajan et al. 2016). Fortunately, thrombolysis is an effective method to treat such diseases (Prilepskii et al. 2018).

Nattokinase (NK) has strong fibrinolytic activity and can treat thrombotic diseases (Yanagisawa et al. 2010; Yoo et al. 2019). The thrombolytic mechanism of NK is diverse. NK cannot only directly dissolve thrombi by interacting with fibrin but also indirectly dissolve thrombi by increasing the levels of hemolytic factors in the body (Fujita et al. 1995). NK is a polypeptide enzyme composed of 275 amino acids, with no disulfide bonds, and has a molecular weight of approximately 28 000 Da. This enzyme can withstand temperatures below 45 °C. At 37 °C, the enzyme activity of NK is relatively stable in the pH range of 4.5 to 8.0, with activity values all above 85%. Compared with other thrombolytic drugs, NK has the advantages of good safety, low production cost and strong fibrinolytic activity and has great clinical application potential. In view of the excellent thrombolytic effect of NK, it has attracted increasing attention from researchers (Lee et al. 2015; Bhatt et al. 2017).

To date, the fermentation process of NK has been gradually optimized, and its yield and thrombolytic activity are increasing (Itaya et al. 2019; Cui et al. 2018). There have been many studies on the pharmaceutical dosage forms of NK. A preparation of NK capsules using sodium polyglutamate and sodium alginate improved the relative activity of enzymes in an acidic environment (Hsieh et al. 2009); NK was also prepared in tablet form and coated with enteric material to avoid stomach acid and improve the bioavailability (Law and Zhang 2007); and NK was prepared as sustained release tablets to extend the treatment time (Yang et al. 2007). There are also new dosage forms such as NK liposomes (Dong et al. 2012) and a NK-loaded self-double-emulsifying drug delivery system (Wang et al. 2015). In this study, sustained release magnetic nanomaterials were used as carriers to prepare NK-MNPs. Under the control of an external magnetic field, these NK-MNPs can be targeted to the thrombus to treat local thrombosis.

2. Investigations and results

2.1. Synthesis and characterization of NK-MNPs

Magnetite materials were obtained by an improved coprecipitation method. NK was loaded on magnetite materials *via* electrostatic interactions and amide linkages. Carboxymethyl chitosan (CMC) and sodium alginate (SA) cannot only improve the storage stability of NK-MNPs but also provide sustained release effects. Magnetite materials were confirmed via X-ray diffraction (XRD) (Fig. 1A). The XRD pattern showed that these magnetite materials contained Fe_3O_4. As shown in Fig. 1B, NK-MNPs and magnetite materials had the same characteristic peaks: amido bond characteristic peaks at approximately 1593 cm^{-1} and 1405 cm^{-1} and a Fe–O signal at approximately 561 cm^{-1}. Simultaneously, the infrared spectroscopy patterns of NK-MNPs and NK had the same characteristic peaks at approximately 1645 cm^{-1}, 1147 cm^{-1}, 998 cm^{-1} and 501 cm^{-1} (Fig. 1B). Magnetite materials loaded with NK were further

characterized by zeta potential and particle size measurements. The mean particle size of NK-MNPs increased from 148.4±5.0 nm (magnetite materials) to 168.9±4.8 nm, and the zeta potential changed from -47.4±0.7 mV to -33.8±0.9 mV. These results confirm the successful preparation of NK-MNPs. The entrapment efficiency was approximately 42%.

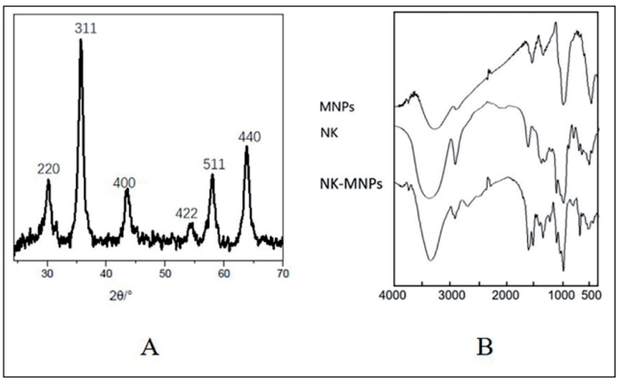

Fig. 1: Characterization of NK-MNPs

2.2. Release behavior

The release behavior results are shown in Fig. 2. In the first 1 h, the release rate was 20.14%, which was less than 40%, and there was no burst release phenomenon. The cumulative release at 72 h was 71.02%, exceeding 70%, indicating that NK was completely released and had a sustained release effect.

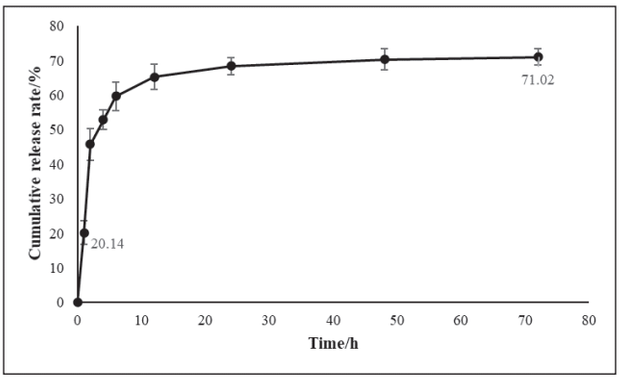

Fig. 2: Release behaviors of NK-MNPs

2.3. Targeting properties

NK-MNPs are magnetic and can gather at a certain location under the action of external magnetic fields. The nanoparticles gathered very quickly in the first hour, after which the speed began to decrease (Fig. 3). The light transmittance reached 87.84% at 24 h, and most of the magnetic substances gathered together, showing good magnetic properties. After 48 h, almost complete gathering had occurred, and the light transmittance was 94.99%.

2.4. Thrombolytic activity in a clot model

The thrombolytic activity of NK-MNPs was tested. The results showed that the blood clot in phosphate-buffered saline (PBS) and magnetic materials solution did not dissolve significantly at 24 h. It was confirmed that the PBS and magnetic materials were not associated with thrombolysis (Fig. 4A and B). By contrast, the thrombi in solutions containing free NK and NK-MNPs were completely dissolved (Fig. 4C and D), which shows that NK can directly dissolve thrombi. The time for the thrombus to completely dissolve in the free NK solution was approximately 10 h, while it was approximately 21 h for the NK-MNP solution (Fig. 4E). Compared with that for free NK, the time for NK-MNPs to dissolve blood clots was significantly longer (P <0.0001).

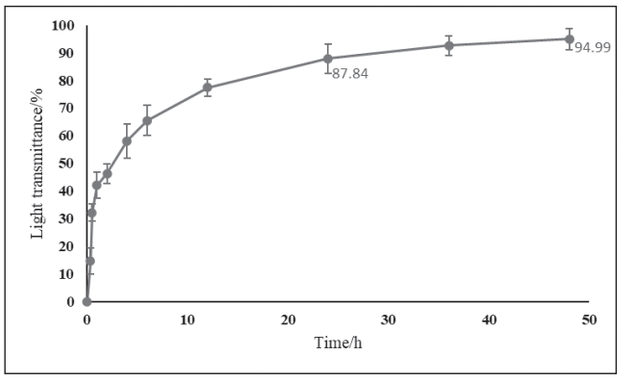

Fig. 3: Magnetic properties

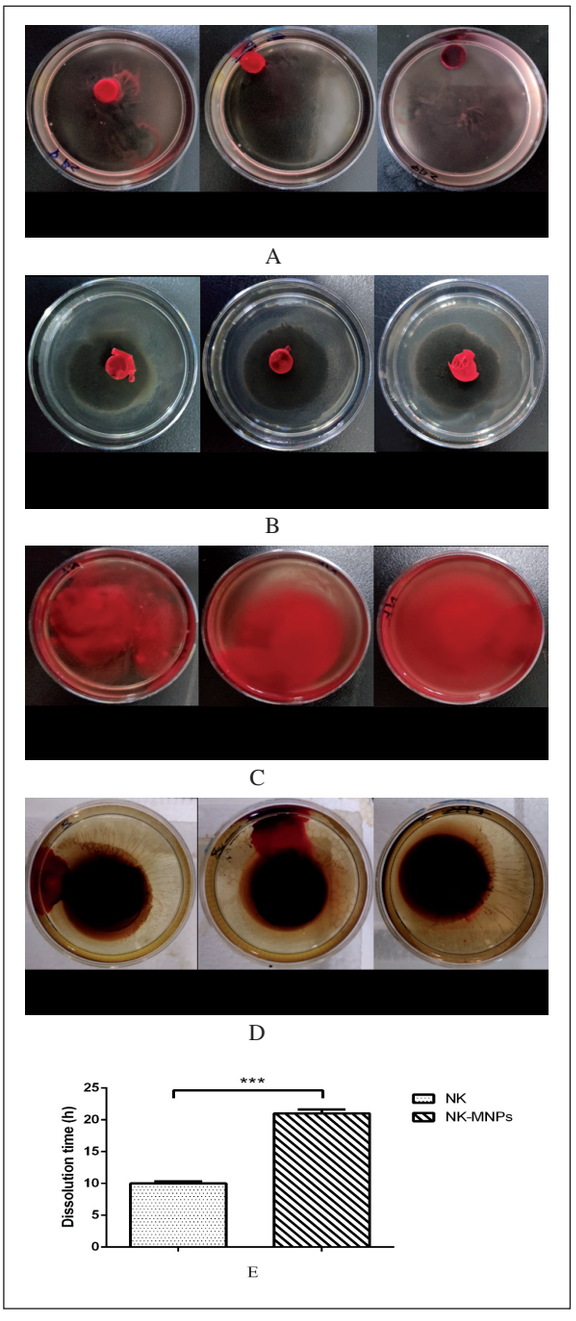

Fig. 4: Blood clot dissolution. A, PBS group; B, magnetic material group; C, free NK group; D, NK-MNPs group. A and B were recorded after 24 h, and C and D were recorded after the blood clot was completely dissolved. E, the time for free NK and NK-MNPs to dissolve blood clots. ***P <0.0001.

2.5. Hemolysis

The hemolysis test was used to investigate whether the drug will affect blood cells. In the hemolysis test, the magnetic material in the experiment itself has a color, which will affect the measured absorbance, i.e, the optical density (OD) value. Therefore, each test group subtracts the absorbance value associated with the cell-free solution. The cells completely ruptured in distilled water, and the solution turned red (Fig. 5A-6). In PBS, the cells sank to the bottom and did not rupture, and the upper solution was clear and colorless (Fig. 5A-5). The hemolysis rate of the magnetic materials was only 0.22%, indicating that magnetic materials did not cause hemolysis (Fig. 5A-4). The hemolysis rate was 0.67% at an enzyme activity of 50 IU/mL (Fig. 5A-1), while it was 3.35% at 150 IU/mL (Fig. 5A-3). These values were all less than 5% and thus did not cause hemolysis. With the increase in the amount of NK-MNPs, the hemolysis rate gradually increased.

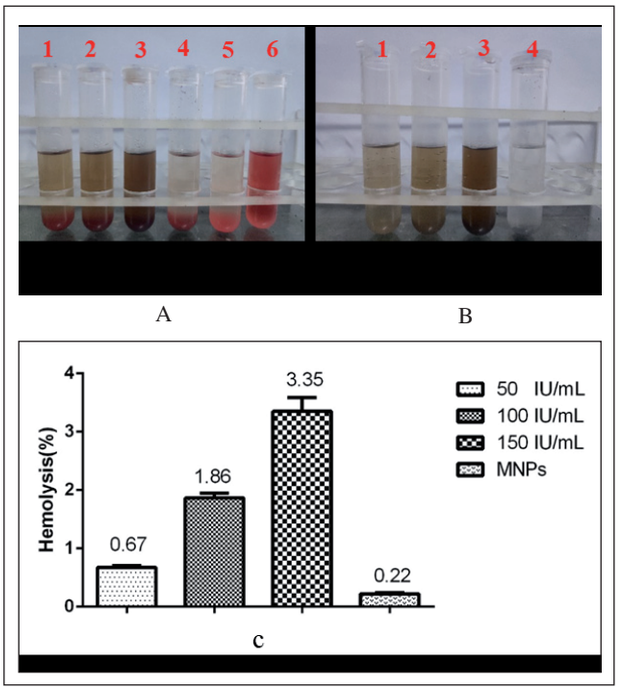

Fig. 5: Hemolysis test. A, 2% erythrocytes: 1-3, NK-MNPs added to reach an enzyme activity of 50, 100 and 150 IU/mL; 4, only magnetic materials added; 5, in PBS; 6, in distilled water; B, lacking 2% erythrocytes: 1-3, NK-MNPs added to reach an enzyme activity of 50, 100 and 150 IU/mL; 4, only magnetic materials added. C, hemolysis rate.

2.6. Storage stability

NK is expected to be developed into a new drug, so storage stability is very important. NK-MNPs retained high activity over 90 days. Specifically, the NK-MNPs retained 99%, 97% and 92% of their initial activity after storage at 4 °C for 30, 60 and 90 days, respectively (Fig. 6). Therefore, NK-MNPs can be stored at 4 °C, and the enzyme activity can be kept above 90% over 90 days.

3. Discussion

Fe_3O_4 is a kind of black iron oxide with excellent magnetic properties and has unique physical and chemical properties (Ebrahimiasl and Azarifar 2019; Kim et al. 2018). This material has a wide range of applications and is used as a magnetic liquid, microwave absorption material, physical targeting carrier, contrast imaging material, etc. There are many preparation methods for Fe_3O_4, including the hydrothermal method, coprecipitation method, sol-gel process, etc. In this study, Fe_3O_4 was synthesized by the coprecipitation method (Pusnik et al. 2016), and 25% ammonia water was used as the precipitant. Compared with other methods, the coprecipitation method does not require complicated equipment. It also has the advantages of mild reaction conditions and high product purity.

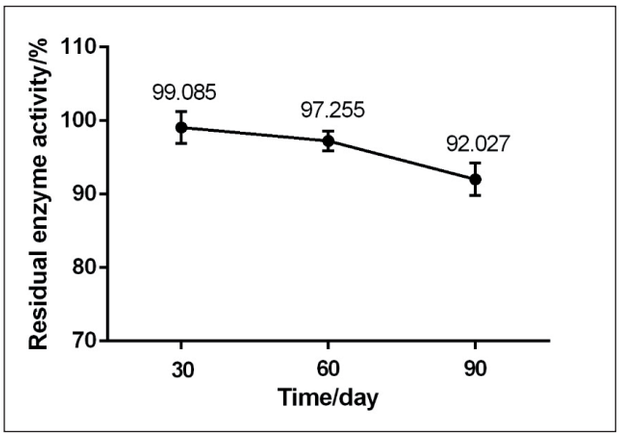

Fig. 6: Storage stability

Changing the size of Fe_3O_4 particles or modifying the structure can result in special paramagnetic and surface effects and small size effects. CMC and SA were used to structurally modify Fe_3O_4 to prepare materials with sustained and controlled release properties. CMC is a derivative of chitosan and can be dissolved in water. This compound is biocompatible and is often used as a drug carrier in microcapsules, microspheres and gels (Shariatinia 2018). Both CMC and SA have a sustained release effect and are very suitable as carriers for NK (Ravichandran and Jayakrishnan 2018).
Compared with free NK, NK-MNPs significantly prolong the time for the blood clot to completely dissolve, further indicating that it has a sustained release effect. The reason for the sustained release is because CMC and calcified SA are both sustained release materials. Additionally, NK may form chemical bonds, such as peptide bonds and ester bonds, with these materials. The magnetic properties of the material are determined by light transmittance. Under an external magnetic field, the NK-MNPs in the petri dish gather, and the OD value of the solution at the edge of the petri dish decreases.

4. Experimental

4.1. Materials

CMC (the degree of deacetylation was more than 95%), SA, 1-hydroxybenzotriazole hydrate (HOB•H_2O), 1-(3-dimethylaminopropyl)-3-ethylcarbodiimide hydrochloride (EDC) (Beijing, China), ferrous chloride tetrahydrate ($FeCl_2$•$4H_2O$), ferric chloride hexahydrate ($FeCl_3$•$6H_2O$), ammonium hydroxide (NH_3•H_2O), calcium chloride ($CaCl_2$), and triethylamine were used (Tianjin, China). All of the reagents were of analytical grade and directly used as received without further purification.

4.2. Synthesis of magnetite materials

Magnetite materials were prepared by the coprecipitation method as previously described, with some modifications (Pusnik et al. 2016). First, 10.0 g CMC was dispersed into 150.0 mL distilled water and stirred (50 °C, 150 r/min) in a magnetic heating stirrer until completely dissolved. Then, 40.0 g $FeCl_3$•$6H_2O$ and 16.0 g $FeCl_2$•$4H_2O$ were added, and the mixture was stirred for an additional 10 min. Next, 25.0 mL 25% NH_3•H_2O was added to the mixture. The reaction continued at 60 °C for 1 h, after which magnetofluid was generated. The solution was cooled to room temperature and deposited overnight. The stirring operation was performed under nitrogen. Then, the solution was dialyzed (10 000 Da MWCO dialysis membrane) against distilled water, which was boiled to remove oxygen under mild stirring for 48 h until unreacted molecules and ions were completely removed. Next, 10.0 g SA was added, and the mixture was stirred for 24 h. Finally, the sample was passed through a 0.22 μm filter and freeze-dried to prepare powder.

4.3. Synthesis of NK-MNPs

NK-MNPs were prepared as described with some modifications (Jiang et al. 2016). First, 60 μL triethylamine, 0.4 g HOBt•H_2O and 0.4 g EDC were dispersed into a 10 mL magnetite material solution and stirred at 0 °C for 0.5 h, after which 0.6 g NK was added. The mixture was stirred at 16 °C for 16 h. Then, 1.0 mL 1% $CaCl_2$ was added. The reaction mixture was continuously stirred at 16 °C for 24 h, followed by extensive dialysis to remove unbound NK. The entrapment efficiency of NK-MNPs was measured using the formula below.

$$\text{Entrapment efficiency} = \frac{m_1}{m_0} \times 100$$

where m0 represents the amount of NK initially added and m1 represents the amount of NK in NK-MNPs.

4.4. Characterization methods

The size and zeta potential of NK-MNPs were determined by a Malvern Nano ZS system. XRD was employed to analyze the crystal structure of the samples and compared with the standard Fe_3O_4 (Rimus et al. 2020). Fourier transform infrared (FTIR) spectroscopy was recorded using an FTIR spectrometer (Spectrum One) (Khatamian et al. 2019).

4.5. In vitro release analysis

The *in vitro* release behavior of NK-MNPs was evaluated in a dialysis bag (50 000 Da, MWCO dialysis membrane). First, 0.08 g NK-MNPs was dispersed in 1.0 mL PBS in a dialysis bag. Then, the filled dialysis bag was placed into 20 mL PBS and placed in a shaker incubator at 37 °C. A 0.5 mL sample was obtained from the outer PBS solution at 1, 2, 4, 6, 12 and 24 h. Later, the thrombolytic activity of NK was determined quantitatively. At the same time, 0.5 mL PBS was replenished into the outside medium to keep the volume constant.

4.6. Targeting properties

The targeting ability was indicated by light transmittance. First, 0.2 g NK-MNPs was placed into a petri dish with a diameter of 6 cm. Then, 15.0 mL PBS (pH 7.4) was added. A cylindrical magnet was placed in the center of the bottom of the petri dish to provide an external magnetic field. A 0.2 mL solution at the edge of the petri dish was taken at 0, 0.3, 0.5, 1, 2, 4, 6, 12, 24, 36, and 48 h, and the absorbance was measured at 560 nm. The light transmittance of NK was measured using the following formula.

$$\text{Light transmittance (\%)} - \frac{A - B}{A} \times 100\%$$

where A is the absorbance value of the solution at 0 h and B is the absorbance value of the solution at a certain hour.

4.7. Thrombolytic activity

An *in vitro* thrombolysis study was performed in a petri dish partly simulating the occlusive thrombus developed in blood vessels (Correa-Paz et al. 2019). Blood was taken from the ear vein of a rabbit and transferred to a 4 mL tube with a pipette. Subsequently, 0.5 mL blood was added to each tube, which naturally clotted into a thrombus at room temperature for 20 h. Next, the thrombus was gently removed with a needle and placed in a 6 cm diameter petri dish. Then, NK-MNPs (in PBS, 600 IU/mL) were added into the petri dish with blood clots, as were PBS, magnetite materials (in PBS) and free NK (in PBS, 600 IU/mL). Afterwards, 15.0 mL PBS was added to a petri dish under which a magnet with a diameter of 2 cm was placed. The dishes were maintained in an air atmosphere at 37 °C, and the time required for each thrombus to completely dissolve was recorded.

4.8. Hemolysis study

The hemocompatibility of NK-MNPs was evaluated through a hemolysis study on red blood cells. According to the Chinese Pharmacopoeia, a 2% (V/V) red blood cell solution was obtained. Fresh mouse blood was collected in a conical flask and stirred gently with a glass rod to remove fibrin. Then, approximately 10 times the amount of saline was added and mixed well. After centrifugation at 1000 r/min for 15 min, the supernatant was removed. The above process was repeated until there was no red in the supernatant. The red blood cells were diluted to 2% (V/V) with normal saline and stored at 4 °C until use.
As shown in the Table, 2% (V/V) erythrocytes, NK-MNPs, magnetic nanomaterials, PBS (negative control), and distilled water (positive control) were added to the tubes. The tubes were mixed gently to avoid artificially breaking the red blood cells. The samples were incubated with red blood cells for 6 h at 37 °C. Then, the OD at 560 nm was measured to examine the samples' hemocompatibility. When the hemolysis rate is higher than 5%, the sample will cause hemolysis (Yuan et al. 2012).
Hemolysis rate (%) = (OD_{sample}-$OD_{negative}$-$OD_{no\ erythrocyte}$) / ($OD_{positive}$-$OD_{negative}$) ×100%

Table: Hemolysis test sample compositions

	1	2	3	4	5	6	7	8	9	10
2% (V/V) Erythrocytes (mL)	2.5	2.5	2.5	2.5	2.5	2.5				
NK-MNPs (IU/mL)	50	100	150				50	100	150	
Magnetite materials (g)				0.05						0.05
Distilled water (mL)						2.5				
PBS (mL)				2.5	2.5		5	5	5	5

4.9. Storage stability of NK-MNPs

The enzyme activity of NK-MNPs was measured at 4 °C for 0, 30, 60 and 90 days. The remaining enzyme activity was calculated by the following formula.
Remaining enzyme activity (%) = 30/60/90 days (enzyme activity) / 0 day (enzyme activity) ×100%
Acknowledgments: This work was supported by the Key R&D Program of Liaoning Province under Grant Nos. 2019JH2/10300041 and 2019JH5/10100041, Shenyang Science and Technology Plan Project under Grant Nos. 17-65-7-00 and 19-302-3-04, and Large-scale Instrument Equipment Sharing Service Platform Capacity Building Fund [grant number kjhx2017028]. This project was supported by the Engineering Laboratory for Molecular Simulation and Designing of Drug Molecules of Liaoning.

Conflicts of interest: The authors declare that there are no conflicts of interest.

References

Baaten CCFMJ, Meacham S, Witt SM, Feijge MAH, Adams DJ, Akkerman J-WN, Cosemans JMEM, Grassi L, Jupe S, Kostadima M, Mattheij NJA, Prins MH, Ramirez-Solis R, Soehnlein O, Swieringa F, Weber C, White JK, Ouwehand WH, Heemskerk JWM (2018) A synthesis approach of mouse studies to identify genes and proteins in arterial thrombosis and bleeding. Carbohydrate Polym 132: 35–46.

Bourcier R, Detraz L, Serfaty JM, Delasalle BG, Mirza M, Derraz I, Toulgoat F, Naggara O, Toquet C, Desal H (2017) MRI Interscanner agreement of the association between the susceptibility vessel sign and histologic composition of thrombi. J Neuroimaging 27: 577–582.

Bhatt PC, Pathak S, Kumar V, Panda BP (2017) Attenuation of neurobehavioral and neurochemical abnormalities in animal model of cognitive deficits of Alzheimer's disease by fermented soybean nanonutraceutical. Inflammopharmacology 26: 105–118.

Cui WJ, Suo FY, Cheng JT, Han LC, Hao W., Guo JL, Zhou ZM (2018) Stepwise modifications of genetic parts reinforce the secretory production of nattokinase in Bacillus subtilis. Microb Biotechnol 11: 930–942.

Correa-Paz C, Poupard MFN, Polo E, Polo E, Rodriguez-Perez M, Taboada P, Iglesias-Rey R, Hervella P, Sobrino T, Vivien D, Castillo J, del Pino P, Campos F, Pelaz B (2019) In vivo ultrasound-activated delivery of recombinant tissue plasminogen activator from the cavity of sub-micrometric capsules. J Control Release 308: 162–171.

Dong XY, Kong FP, Yuan GY, Wei F, Jiang ML, Li GM, Wang Z, Zhao YD, Chen H (2012) Optimisation of preparation conditions and properties of phytosterol liposome-encapsulating nattokinase. Nat Prod Res 26: 548–556.

Ebrahimiasl H, Azarifar D (2019) Copper-based Schiff Base Complex Immobilized on Core-shell Fe_3O_4@SiO_2 as a magnetically recyclable and highly efficient nanocatalyst for green synthesis of 2-amino-4H-chromene derivatives. Appl Organometal Chem 34: e5359.

Fujita M, Ito Y, Hong K, Nishimuro S (1995) Characterization of nattokinase-degraded products from human fibrinogen or cross-linked fibrin. Fibrinolysis 9: 157–164.

Govindarajan V, Rakesh V, Reifman J, Mitrophanov AY (2016) Computational study of thrombus formation and clotting factor effects under venous Flow Conditions. Biophys J 110: 1869–1885.

Hsieh CW, Lu WC, Hsieh WC, Huang YP, Lai CH, Ko WC (2009) Improvement of the stability of nattokinase using g-polyglutamic acid as a coating material for microencapsulation. LWT-Food Sci Technol 42: 144–149.

Itaya M, Nagasaku M, Shimada T, Ohtani N, Shiwa Y, Yoshikawa H, Kaneko S, Tomita M, Sato M (2019) Stable and efficient delivery of DNA to Bacillus subtilis (natto) using pLS20 conjugational transfer plasmids. FEMS Microbiol Lett 366(4).

Jiang JF, Chen YZ, Wang W, Cui BD, Wan NW (2016) Synthesis of superparamagnetic carboxymethyl chitosan/sodium alginate nanosphere and its application for immobilizing α-amylase. Carbohydrate Polym 151: 600–605.

Khatamian M, Divband B, Shahi R (2019) Ultrasound assisted co-precipitation synthesis of Fe_3O_4/bentonite nanocomposite: Performance for nitrate, BOD and COD water treatment. J Water Proc Engin 31: 100870.

Kim J, Tran VT, Oh S, Kim C-S, Hong JC, Kim S, Joo Y-S, Mun S, Kim M-H, Jung J-W, Lee J, Kang YS, Koo J-W, Lee J (2018) Scalable solvothermal synthesis of superparamagnetic Fe_3O_4 nanoclusters for bioseparation and theragnostic probes. ACS Appl Mater Probes 10: 41935–41946.

Lee W, Kim MA, Park I, Hwang JS, Na M, Bae JS (2017) Novel direct factor Xa inhibitory compounds from Tenebrio molitor with anti-platelet aggregation activity. Food Chem Toxicol 109: 19–27.

Lee BH, Lai YS, Wu SC (2015) Antioxidation, angiotensin converting enzyme inhibition activity, nattokinase, and antihypertension of Bacillus subtilis (natto)-fermented pigeon pea. J Food Drug Anal 23: 750–757.

Law D, Zhang Z (2007) Stabilization and target delivery of nattokinase using compression coating. Drug Devel Ind Pharm 33: 495–503.

Prilepskii AY, Fakhardo AF, Drozdov TAS, Vinogradov VV, Dudanov IP, Shtil AA, Bel'tyukov PP, Shibeko AM, Koltsova EM, Nechipurenko DY (2018) Urokinase-conjugated magnetite nanoparticles as a promising drug delivery system for targeted thrombolysis: synthesis and preclinical evaluation. ACS Appl Mater Interfaces 10: 36764–36775.

Pusnik K, Gorsal T, Drofenik M, Makovec D (2016) Synthesis of aqueous suspensions of magnetic nanoparticles with the co-precipitation of iron ions in the presence of aspartic acid. J Magnet Magnet Mat 413: 65–75.

Rimus Liandi A, Tri Yunarti R, Fajri Nurmawan M, Herry Cahyana A (2020) The utilization of Fe_3O_4 nanocatalyst in modifying cinnamaldehyde compound to synthesis 2-amino-4H-chromene derivative. Materials Today: Proceedings 22: 193–198.

Ravichandran V, Jayakrishnan A (2018) Synthesis and evaluation of anti-fungal activities of sodium alginate-amphotericin B conjugates. Int J Biol Macromol 108: 1101–1109.

Shariatinia Z (2018) Carboxymethyl chitosan: Properties and biomedical applications. Int J Biol Macromol 120: 1406–1419.

Wang XN, Jiang SF, Wang XY, Liao J, Yin ZN (2015) Preparation and evaluation of nattokinase-loaded self-double-emulsifying drug delivery system. Asian J Pharm Sci 10: 386–395.

Wu H, Wang H, Xu F, Chen JP, Duan LL, Zhang FJ (2019) Acute toxicity and genotoxicity evaluations of nattokinase, a promising agent for cardiovascular diseases prevention. Regulat Toxicol Pharmacol 103: 205–209.

Yanagisawa Y, Chatake T, Chiba-Kamoshida K, Naito S, Ohsugi T, Sumi H, Yasuda I, Morimoto Y (2010) Purification, crystallization and preliminary X-ray diffraction experiment of nattokinase from Bacillus subtilis natto. Struct Biol Cryst Comm 66: 1670–1673.

Yoo HJ, Kim M, Kim M, Lee A, Jin C, Lee SP, Kim TS, Lee SH, Lee JH (2019) The effects of nattokinase supplementation on collagen-epinephrine closure time, prothrombin time and activated partial thromboplastin time in nondiabetic and hypercholesterolemic subjects. Food Function 10: 2888–2893.

Yang C, Yin ZN, Yu GL, Zou Q (2007) Preparation and sustained release factors of nattokinase sustained-release tablets. Chin J New Drugs 16: 547–550.
Yuan J, Yang J, Zhuang ZH, Yang YL, Lin L, Wang SH (2012) Thrombolytic effects of Douchi fibrinolytic enzyme from Bacillus subtilis LD-8547 in vitro and in vivo. BMC Biotechnol 12: 2–9.